Original Article

Correlation between cardiac and hepatic native T1 value and myocardial late gadolinium enhancement in children with Kawasaki disease

Shengkun Peng[1,2#^], Lingyi Wen[1,3#], Zhongqin Zhou[1,3#], Shan Huang[1,3], Lei Hu[1,3], Shiganmo Azhe[1,3], Chuan Wang[4], Nanjun Zhang[4], Meining Chen[5], Kaiyu Zhou[4*], Yingkun Guo[1,3,6*]

[1]Department of Radiology, West China Second University Hospital, Sichuan University, Chengdu, China; [2]Department of Radiology, Sichuan Academy of Medical Sciences and Sichuan Provincial People's Hospital, University of Electronic Science and Technology of China, Chengdu, China; [3]Key Laboratory of Birth Defects and Related Diseases of Women and Children (Sichuan University), Ministry of Education, West China Second University Hospital, Sichuan University, Chengdu, China; [4]Department of Pediatric Cardiology, West China Second University Hospital, Sichuan University, Chengdu, China; [5]MR Scientific Marketing, Siemens Healthineers, Chengdu, China; [6]Key Laboratory of Development and Diseases of Women and Children of Sichuan Province, West China Second University Hospital, Sichuan University, Chengdu, China

Contributions: (I) Conception and design: S Peng, Y Guo, L Wen; (II) Administrative support: K Zhou, C Wang; (III) Provision of study materials or patients: Y Guo, K Zhou, C Wang, L Wen; (IV) Collection and assembly of data: S Peng, Z Zhou, S Azhe, L Hu, S Huang, N Zhang; (V) Data analysis and interpretation: S Peng, Z Zhou; (VI) Manuscript writing: All authors; (VII) Final approval of manuscript: All authors.

[#]These authors contributed equally to this work.

[*]These authors contributed equally to this work.

Correspondence to: Kaiyu Zhou, PhD. Department of Pediatric Cardiology, West China Second University Hospital, Sichuan University, No. 20, Section 3, Renmin South Road, Wuhou District, Chengdu 610041, China. Email: kaiyuzhou313@163.com; Yingkun Guo, PhD. Key Laboratory of Birth Defects and Related Diseases of Women and Children (Sichuan University), Ministry of Education, West China Second University Hospital, Sichuan University, Chengdu, China; Key Laboratory of Development and Diseases of Women and Children of Sichuan Province, West China Second University Hospital, Sichuan University, Chengdu, China; Department of Radiology, West China Second University Hospital, Sichuan University, No. 20, Section 3, Renmin South Road, Wuhou District, Chengdu 610041, China. Email: gykpanda@163.com.

Background: Kawasaki disease (KD) is an acute febrile illness and systemic vasculitis of unknown etiology that predominantly affects young children. The objective of this study was to investigate the correlation between myocardial and hepatic native T1 value and myocardial late gadolinium enhancement (LGE) in pediatric patients with KD.

Methods: In this cross-sectional retrospective study, 115 KD patients (50 in the acute phase, 65 in the chronic phase) and 40 age- and gender-matched controls underwent cardiac magnetic resonance (CMR) imaging with T1 mapping and LGE sequences. KD patients were subgrouped based on the myocardial LGE. Cardiac and hepatic T1 value as well as laboratory tests were also analyzed.

Results: Both cardiac and hepatic T1 value were significantly elevated in KD patients compared to controls, with the highest values noted in the acute phase (myocardial 1,393±70, 1,345±65, 1,303±62 ms; hepatic 813±25, 787±29, 758±38 ms; P=0.001, P=0.001, respectively). KD patients with myocardial LGE had significantly higher myocardial and hepatic T1 value in both the acute (1,442±66, 1,381±67 ms; 836±47, 803±30 ms, P=0.048, P=0.013, respectively) and chronic phases (myocardial 1,393±91, 1,331±50 ms; hepatic 811±39, 780±21 ms, P=0.012, P=0.001, respectively). Multivariate analysis demonstrated a significant

^ ORCID: 0000-0001-5624-2816.

correlation between the disease phase, albumin, and hepatic T1 value in KD patients. The combined of myocardial and hepatic T1 value significantly enhances the diagnostic performance of myocardial LGE, increasing the area under the curve (AUC) from 0.773 to 0.881 (P=0.013).

Conclusions: Elevated myocardial and hepatic T1 values correlate with myocardial LGE in KD, highlighting systemic involvement. The integration of these T1 values enhances the non-invasive diagnosis of myocardial involvement in KD, demonstrating their utility in assessing disease severity and progression.

Keywords: Kawasaki disease (KD); myocardial late gadolinium enhancement (myocardial LGE); T1 mapping; cardiac magnetic resonance (CMR); hepatic assessment

Submitted Apr 18, 2024. Accepted for publication Jan 03, 2025. Published online Feb 26, 2025.
doi: 10.21037/qims-24-791
View this article at: https://dx.doi.org/10.21037/qims-24-791

Introduction

Kawasaki disease (KD) is the most prevalent acquired heart disease among children in developed nations (1). It primarily affects medium-sized arteries and can be accompanied by coronary artery (CA) involvement (2). Our current understanding of myocardial injury in pediatric KD comes primarily from autopsy studies and endomyocardial biopsy (EMB) findings (3,4). Studies have revealed that during the acute phase, the myocardium shows inflammatory cell infiltration, interstitial fibrosis, and structural disarray. Similarly, liver examinations during this phase demonstrate inflammatory changes affecting portal areas, bile ducts, and sinusoids. The chronic stage typically shows marked hepatic steatosis with reduced inflammation (3,4). Although valuable, these post-mortem findings may not fully represent the dynamic nature of organ involvement in living patients. Liver dysfunction is commonly observed through abnormal liver panel tests in KD patients, yet a critical knowledge gap exists regarding the relationship between hepatic and cardiac manifestations. Cardiac magnetic resonance (CMR) imaging has introduced 2 key diagnostic tools: (I) late gadolinium enhancement (LGE), which involves imaging the heart at specific time points (typically 10–20 minutes after the injection of gadolinium contrast agent) to highlight areas of myocardial pathology. In LGE imaging, healthy myocardium typically appears as low signal, whereas damaged or fibrotic myocardial regions absorb the contrast agent and display high signal (5). The detection of LGE has significant clinical implications, as it linked with an increased risk of mortality, sudden cardiac death, and arrhythmias in various adult heart conditions, including ischemic and nonischemic cardiomyopathies, myocarditis, as well as stenosis (6-9). In KD patients, LGE in the myocardium indicates fibrotic remodeling, which along with microvascular dysfunction, leads to decreased myocardial function (10). (II) T1 mapping is an advanced magnetic resonance imaging (MRI) technique that measures tissue health. T1 mapping detects subtle myocardial changes unidentifiable through conventional imaging. Elevated T1 values indicate tissue damage, enabling early detection of cardiac involvement in KD, even when standard imaging appears normal (11). The heart and liver closely affect each other in 2 ways. The heart releases chemicals such as sPLA2 that influence liver metabolism and inflammation. Meanwhile, liver problems can harm heart function. When either organ becomes diseased, it can create a harmful cycle that makes both organs worse. This close connection means doctors need to consider both the heart and liver when treating patients (12-14). Recent advances have successfully extended T1 mapping to evaluate liver tissue, offering insights into liver health without additional testing (15). Studies demonstrate that liver T1 mapping helps to assess heart failure severity and accurately reflects liver tissue scarring (16,17). Concurrently, research has validated the efficacy of hepatic T1 mapping in stratifying patients with idiopathic dilated cardiomyopathy into cohorts, with and without congestive heart failure (15). Given these advances in imaging technology and the current gaps in understanding KD's multi-organ effects, our study aimed to comprehensively evaluate both cardiac and hepatic involvement in pediatric KD patients using CMR. Specifically, investigated how T1 values in heart and liver tissue correlate with the presence of cardiac LGE, potentially providing new insights into the

relationship between cardiac and hepatic manifestations of this important childhood disease. We present this article in accordance with the STROBE reporting checklist (available at https://qims.amegroups.com/article/view/10.21037/qims-24-791/rc).

Methods

Population

From September 2017 to February 2023, 115 patients diagnosed with KD were retrospectively enrolled at the West China Second Hospital of Sichuan University. The calculated sample size for this study was 112. This sample size was based on a 95% confidence level (α =0.05) and a 90% statistical power (β =0.10) (Appendix 1). The patients were diagnosed with KD in accordance with the American Heart Association (AHA) guideline guidelines. All patients underwent CMR imaging as part of the study protocol. Patients with pre-existing cardiomyopathy, congenital heart disease, recurrent KD, or poor image quality were excluded from the analysis (Figure S1). Clinical data collected for each patient included height, weight, intravenous immunoglobulin (IVIG) treatment, and IVIG resistance. The disease course of KD patients was categorized into 2 distinct phases: the acute phase, which extended from the onset of fever up to the 40th day, and the chronic phase, starting from the 41st day onwards (18). The day of initial fever onset was denoted as day 1. Accordingly, the patient cohort divided into 50 patients in the acute phase and 65 in the chronic phase. Additionally, 40 age- and gender-matched individuals initially suspected of having cardiovascular disease but subsequently confirmed to be normal served as controls. This study was conducted in accordance with the Declaration of Helsinki (as revised in 2013). The study was approved by the Ethics Committee of Sichuan University (No. K2019058). Written informed consent was provided by each patient's legal guardian before enrollment. We collected laboratory data including routine blood tests and biochemical markers, within 3 days of hospital admission (prior to initiating IVIG treatment, if administered). For variables with missing laboratory data (with a missing rate of 20–28%), multiple imputation was performed using the MICE package in R language (R Foundation for Statistical Computing, Vienna, Austria) with the classification and regression trees (CART) method to accurately estimate missing values and ensure the integrity of our analyses.

CMR imaging protocol

All CMR scans were performed using a clinical 3.0 T MR scanner (MAGNETOM Skyra; Siemens Healthineers, Erlangen, Germany) equipped with an 18-channel receiver coil. The CMR protocols encompassed cine imaging, native T1 mapping, as well as LGE sequences (19). Native T1 mapping was acquired using a modified Look-Locker inversion recovery (MOLLI) sequence with motion correction across 3 short-axis planes (basal, mid, and apical) of the left ventricular (LV) myocardium. The MOLLI scanning parameters were set as follows: flip angle (FA) =35°, repetition time (TR) =3.90 ms, echo time (TE) =1.74 ms, slice thickness =6.0 mm, matrix =139×192, and field of view (FOV) =280×224 mm^2. For heart rates between 60 and 80 bpm, the scanning model used was 5(3)3; for heart rates of 80–120 bpm, the model was 5(5)3; and for heart rates exceeding 120 bpm, the model was 7(5)1. These protocols ensured adequate pulse recovery time for accurate T1 mapping (20). The diaphragmatic-navigated cardiac magnetic resonance angiography (CMRA) was performed using gradient echo sequence (21). LGE images were acquired 5–8 minutes following the intravenous administration of gadolinium (Gadovist, Bayer Healthcare, Berlin, Germany) at a dose of 0.15 mmol/kg. These images were acquired using a single-shot phase-sensitive inversion recovery (PSIR) sequence with optimized parameters: TE of 1.09 ms, TR of 2.55 ms, FA of 55°, slice thickness of 6 mm, matrix size of 116×192, and FOV ranging from 340–360 × 340–360 mm^2.

CMR image analysis

CMR analysis was conducted by 2 experienced clinical physicians, S.P. and Z.Z., with 11 and 6 years of experience in CMR diagnosis, respectively, using commercially available software (cvi42; Circle Cardiovascular Imaging Inc., Calgary, Alberta, Canada). In accordance with current guidelines (20,22), LV functional parameters, including left ventricular ejection fraction (LVEF), end-diastolic volume index (EDVI), end-systolic volume index (ESVI), and left ventricular mass index (LVMI), were derived by defining the contours of endocardial and epicardial borders on short-axis cine images. After excluding segments influenced by artifacts, the global native T1 value for the

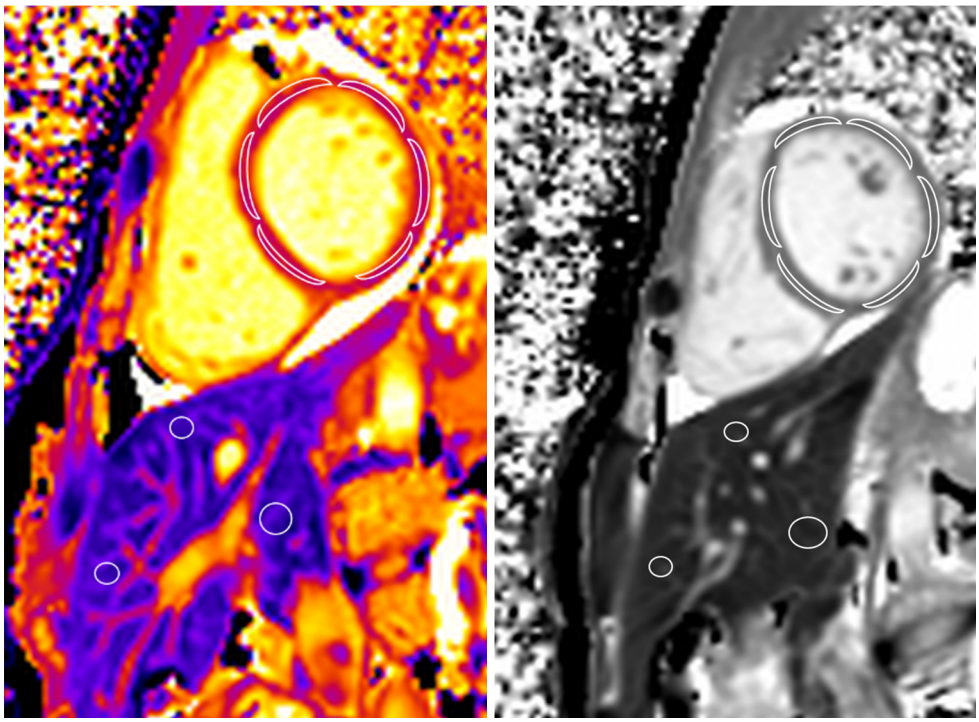

Figure 1 T1 mapping analysis. Upper ROI: cardiac native T1. The manually delineated white lines represent the ROIs between the endocardial and the epicardial myocardium. Lower ROIs: hepatic native T1. Three ROIs placed in the liver, avoiding visible blood vessels, bile ducts, and selecting healthy liver parenchyma outside of any lesions (lower panel). The left panel displays a color-coded T1 map, while the right panel shows the corresponding grayscale image. ROIs, regions of interest.

entire LV myocardium was computed based on the mean of the remaining segments (*Figure 1*). The presence and pattern of LGE were visually assessed by an expert reader, L.W., with 11 years of experience in CMR diagnosis, according to the AHA 16-segment model. The number of affected segments was also noted. LGE was assessed in each myocardial segment as either negative or positive, independent of T1 analysis. A patient with LGE in at least one segment was considered to have cardiac involvement. Absence of enhancement indicated a KD patient without cardiac involvement. Hepatic T1 mapping was derived from a MOLLI sequence, which was performed on a cardiac short-axis slice, to acquire the T1 relaxation times of the liver. To obtain the T1 mapping, 3 regions of interest (ROIs) were drawn in different areas of the liver, including regions near the diaphragm, intermediate regions near the hepatic hilum, and the posterior and peripheral regions of the liver (16). The average of the 3 ROIs was taken as the liver T1 value. We obtained the internal diameter and location of CA dilation from CMRA images. Subsequently, we incorporated variables such as CA dilation diameter, gender, height, and weight of KD patients into a lambda-mu-sigma derived model to calculate the coronary Z-score (23).

Reproducibility of T1 mapping

A total of 21 randomly selected cases from the enrolled patients underwent repeated measurements for intra-observer variability, conducted by the same observer (S.P.) after a 3-week interval. Furthermore, inter-observer variability was evaluated by a second independent observer (Z.Z.), who was blinded to the participants' information. Inter-observer variability for reproducibility was assessed using Bland-Altman analysis.

Statistical analysis

Statistical analyses were performed using the software SPSS 26.0 (IBM Corp., Armonk, NY, USA), GraphPad Prism 9 (GraphPad Software, San Diego, CA, USA), MedCalc v 15.6.1 (MedCalc Software, Ostend, Belgium),

Table 1 Baseline characteristics of normal controls and KD patients

Characteristics	Controls (n=40)	KD (acute phase) (n=50)	KD (chronic phase) (n=65)	P value
Baseline characteristics				
Age at CMR (years)	4.71±2.29	4.96±3.04	5.66±2.37	0.083
Age at onset (years)	N/A	4.59±2.84	4.38±2.36	0.618
Male	29 (72.5)	32 (64.0)	40 (61.5)	0.561
BSA (m^2)	0.77±0.22	0.82±0.27	0.79±0.20	0.884
IVIG treatment	N/A	44 (88.0)	57 (87.7)	0.960
IVIG resistant	N/A	14 (28.0)	23 (35.4)	0.401
HR (beats/min)	92.40±13.39	94.28±17.08	94.14±16.72	0.828
LV function				
LVEF (%)	59.38±9.21	58.80±7.33	59.00±10.40	0.728
LVEDVI (mL/m^2)	55.6 (44.60–74.68)	54.2 (32.14–79.81)†	69.7 (58.54–98.12)‡	0.001
LVESVI (mL/m^2)	23.51 (18.04–29.82)	23.83 (14.18–29.96)†	38.46 (21.1–30.7)‡	0.001

Values are n (%) for categorical variables, median (interquartile range) for continuous variables, or mean ± standard deviation. Statistical analysis was performed using one-way analysis of variance for normally distributed variables. Kruskal-Wallis test for non-normally distributed variables († and ‡). A P value <0.05 was considered statistically significant. †, P<0.05 when compared with KD in acute phase; ‡, P<0.05 when compared with controls. KD, Kawasaki disease; CMR, cardiac magnetic resonance; N/A, not available; BSA, body surface area; IVIG, intravenous immunoglobulin; HR, heart rate; LV, left ventricle; LVEF, LV ejection fraction; LVESVI, LV end-systolic volume index; LVEDVI, LV end-diastolic volume index.

and R studio (version 4.1.2, http://www.r-project.org/). For variables with missing data ranging between 20% and 35%, multiple imputation techniques were applied using the mice package in R, employing the classification and regression tree method to estimate missing values. The normality of continuous variables was assessed using the Kolmogorov-Smirnov test, and the homogeneity of variances was assessed using the Levene test. Normally distributed continuous variables were reported as mean ± standard deviation (SD), and non-normally distributed variables were presented as median and interquartile range (IQR). Categorical data were presented as frequencies and percentages. The Kruskal-Wallis test was used to compare demographic data between KD patients and the healthy controls. One-way analysis of variance (ANOVA) was performed to compare the native T1 value and LV function among different groups and subgroups with post hoc analysis performed using the least significant difference test for the P value less than 0.05. Statistical analysis was performed using one-way ANOVA to evaluate overall differences among groups. When ANOVA indicated significance (P<0.05), the least-significant difference (LSD) test was used for post-hoc comparisons. Spearman's rank correlation was used to evaluate the correlation between laboratory data and hepatic T1 value. Univariate and multivariate linear regression analyses explored factors influencing hepatic T1 value, and we used a stepwise backward elimination method to select variables. Univariate and multivariate binary logistic regression analyses were used to investigate factors affecting the presence of myocardial LGE. We applied an R^2-based optimal model selection approach, aiming to identify the model that maximized explanatory power while avoiding overfitting. Receiver operating characteristic (ROC) curves were generated to form 4 models based on different inclusion factors, with ROC curve performance assessed using the Delong test. The intraclass correlation coefficient (ICC) was used to assess the consistency of native T1 value between and within observers. Statistical significance was considered for all tests when 2-tailed P values were less than 0.05.

Results

Participants baseline characteristics

The baseline characteristics of the participants are

Table 2 Myocardial and hepatic T1 value in KD patients at different disease phases

Native T1	Controls	KD (acute phase)			KD (chronic phase)		
		All (n=50)	LGE$^+$ (n=10)	LGE$^-$ (n=40)	All (n=65)	LGE$^+$ (n=14)	LGE$^-$ (n=51)
Myocardial (ms)	1,303.33±61.83	1,393.05±70.67†	1,441.88±66.46†‡	1,380.84±67.02†	1,344.55±65.42†‡	1,392.51±90.74†‡	1,331.39±50.16†
Hepatic (ms)	758.37±38.29	812.92±25.14†	835.99±47.29†‡	803.24±29.95†	786.82±28.61†‡	811.21±38.97†‡	780.12±20.98†

Data are presented as mean ± standard deviation. Statistical analysis was performed using one-way analysis of variance for normally distributed variables († and ‡). A P value <0.05 was considered statistically significant. †, P<0.05 when compared with controls; ‡, P<0.05 when compared with KD in acute phase. KD, Kawasaki disease; LGE, late gadolinium enhancement.

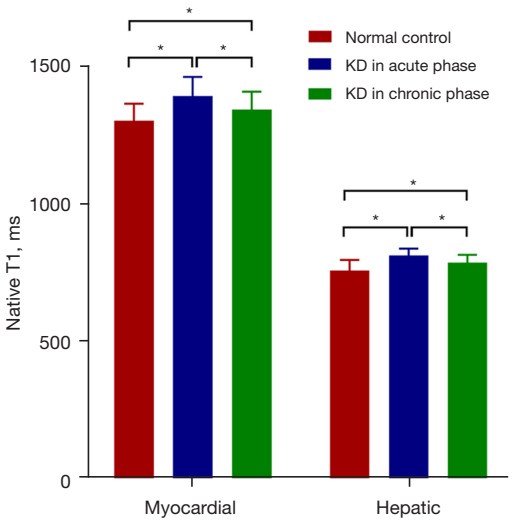

Figure 2 Myocardial and hepatic T1 value among controls and patients with different courses of KD. *, significant difference between any 2 groups. KD, Kawasaki disease.

summarized in *Table 1*. The study included 40 normal controls, comprising 29 males with an average age of 4.71±2.29 years. Among KD patients, 50 were in the acute phase (32 males, average age 4.96±3.04 years) and 65 were in the chronic phase (40 males, average age 5.66±2.37 years). No significant differences were found between normal controls and KD patients in terms of age at CMR, age at onset, sex, body surface area (BSA), heart rate, or LVEF across both acute and chronic phases. KD patients in the acute phase exhibited higher left ventricular end-systolic volume index (LVESVI) and left ventricular end-diastolic volume index (LVEDVI) compared to those in the chronic phase (LVEDVI 69.7, 54.2 mL/m^2; LVESVI 38.5, 23.8 mL/m^2, all P<0.05) (Figures S2-S4). The percentages of IVIG treatment and IVIG resistance showed no significant differences between the acute and chronic phases. Patients were also categorized into positive (n=24) and negative (n=91) subgroups based on the presence or absence of LGE in contrast-enhanced CMR.

Dilated CA and LGE patterns

In the acute phase, a total of 50 KD patients were studied, of whom 10 patients presented with LGE-positive findings. The right coronary artery (RCA) was affected in 4 patients, the left main coronary artery (LM) in 2 patients, the left anterior descending artery (LAD) in 3 patients, and the left circumflex artery (LCX) in 3 patients. The affected CA territories matched the LGE-positive regions in 2 patients (20%). In the chronic phase, a total of 65 KD patients were studied, among whom 14 patients exhibited LGE-positive findings. The RCA was affected in 12 patients, the LM in 8 patients, the LAD in 10 patients, and the LCX in 4 patients. The affected CA territories corresponded to the LGE-positive regions in 11 patients (78.57%) (Table S1 and Figure S5).

Comparison of myocardial and hepatic T1 value in different phases

Myocardial T1 value was highest in acute phase KD patients, followed by those in the chronic phase, and was lowest in the control group (1,393.05±70.67 *vs.* 1,344.55±65.42 *vs.* 1,303.33±61.83 ms, P<0.01) (*Table 2*). A similar pattern was observed for hepatic T1 value (812.92±25.14 *vs.* 786.82±28.61 *vs.* 758.37±38.29 ms, P<0.01) (*Figure 2*). Within the myocardial LGE subgroups, acute phase KD patients with LGE$^+$ demonstrated higher T1 value compared to those with LGE$^-$ (1,441.88±66.46 *vs.* 1,380.84±67.02 ms, P<0.01), and this trend continued in the chronic phase (1,392.51±90.74 *vs.* 1,331.39±50.16 ms, P<0.01) (*Figure 3*). Similarly, hepatic T1 value was significantly higher in LGE$^+$ patients during both the acute (835.99±47.29

vs. 803.24±29.95 ms, P<0.01) and chronic phases (811.21±38.97 *vs.* 780.12±20.98 ms, P<0.01). Bivariate correlation analysis revealed a positive correlation between myocardial and hepatic T1 value (r=0.249, P=0.007).

Univariate and multiple linear regression analysis for determinants of hepatic T1 value with KD patients

Laboratory parameters, including white blood cell (WBC) count, neutrophil (NEUT) count, C-reactive protein (CRP), albumin (ALB), lymphocyte count (LYM), alanine aminotransferase (ALT), aspartate aminotransferase (AST), and total bilirubin (TBIL), exhibited significant correlations with hepatic native T1 value in the acute phase (r=0.328, r=0.342, r=0.485, r=–0.318, r=–0.320, r=–0.505, r=–0.320, and r=–0.358, respectively; all P<0.05) (*Figure 4*). Multiple linear regression analysis, adjusted for clinical characteristics and laboratory parameters, revealed that CRP was independently correlated with hepatic native T1 value during the acute phase (β =0.485, P=0.015, model R^2=0.236). There was a significant correlation observed between LYM (β =–0.320, P=0.023) and ALB (β =–0.318, P=0.025) levels with hepatic native T1 value in the chronic phase. Nevertheless, the multiple linear regression model did not demonstrate statistically significant associations in the chronic phase. After adjusting for clinical characteristics (age, LVEF, Z-score, and disease phase) and laboratory parameters (ALB and LYM), multivariate analysis demonstrated a significant correlation between disease phase and ALB with hepatic T1 value in both phases (disease phase: β =–0.403, P=0.001; ALB: β =–0.218, P=0.010; model R^2=0.221) (*Table 3*).

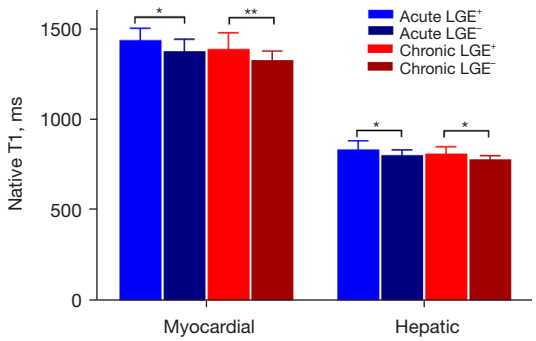

Figure 3 Myocardial and hepatic T1 value between patients with LGE$^+$ and LGE$^-$ in different courses of KD. *, P<0.05; **, P<0.01. LGE, late gadolinium enhancement; KD, Kawasaki disease.

Univariable and multivariable logistic regression analysis for myocardial LGE in KD patients

Four models are depicted in *Table 4* and *Figure 5*, each incorporating different sets of variables to predict myocardial LGE. Model 1, including Z-score and sodium levels (Na^+), showed an area under the curve (AUC) of 0.773. The addition of LVEF in Model 2 [Z-score + Na^+ + LVEF]

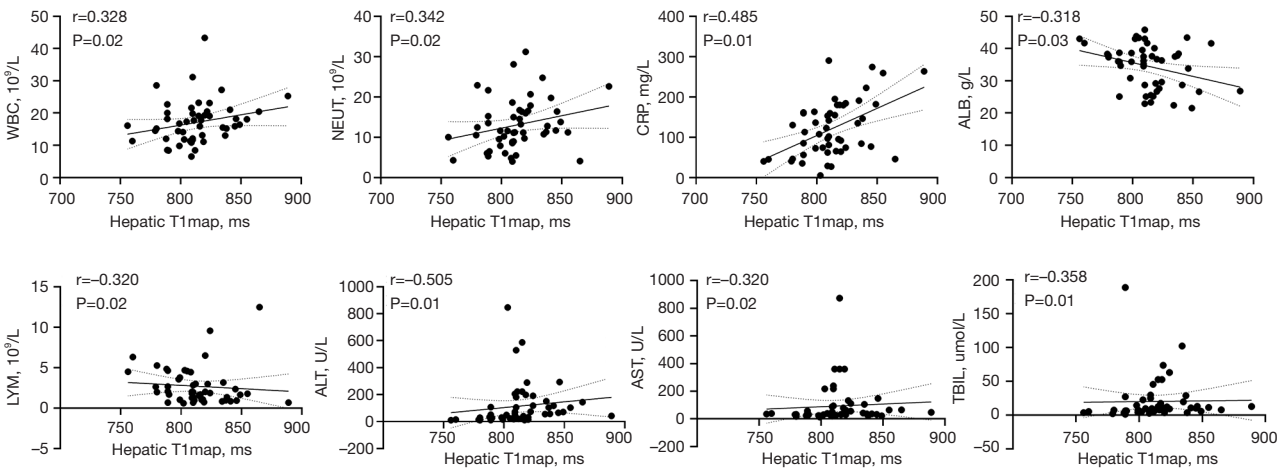

Figure 4 Correlation of laboratory parameters with hepatic native T1 value in acute phase. WBC, white blood cell; NEUT, neutrophil; CRP, C-reactive protein; ALB, albumin; LYM, lymphocyte count; ALT, alanine aminotransferase; AST, aspartate aminotransferase; TBIL, total bilirubin.

Table 3 Univariable and multivariable linear regression analysis of hepatic native T1 value in all KD patients (n=115)

Variables	Univariable		Multivariable		Adjusted R^2
	r	P value	β	P value	
Disease phase	−0.433	0.001	−0.403	0.001	0.221
ALB	−0.298	0.003	−0.218	0.010	
Age	0.418	0.001	–	–	
LYM	−0.336	0.001	–	–	
Z-score	−0.045	0.630	–	–	
LVEF	−0.174	0.063	–	–	

KD, Kawasaki disease; ALB, albumin; LYM, lymphocyte count; LVEF, left ventricular ejection fraction.

Table 4 Univariable and multivariable logistic regression analysis for myocardial LGE in KD patients

Variable	Model 1			Model 2			Model 3			Model 4		
	OR (95% CI)	P value	R^2	OR (95% CI)	P value	R^2	OR (95% CI)	P value	R^2	OR (95% CI)	P value	R^2
Z-score	1.20 (1.08–1.32)	0.001	0.250	1.18 (1.05–1.32)	0.005	0.358	1.18 (1.05–1.34)	0.006	0.431	1.23 (1.08–1.40)	0.002	0.521
Na^+	0.85 (0.73–0.96)	0.010		0.80 (0.69–0.93)	0.003		0.80 (0.68–0.93)	0.003		0.84 (0.72–1.00)	0.037	
LVEF	–	–		0.91 (0.85–0.98)	0.007		0.93 (0.86–1.00)	0.039		0.93 (0.87–1.00)	0.048	
Myocardial T1 map	–	–		–	–		1.01 (1.00–1.02)	0.010		1.01 (1.00–1.02)	0.034	
Hepatic T1 map	–	–		–	–		–	–		1.04 (1.01–1.06)	0.005	

Model 1: include Z-score and Na+. Model 2: Model 1 + LVEF. Model 3: Model 2 + myocardial T1 map. Model 4: Model 3 + hepatic T1 map. LGE, late gadolinium enhancement; KD, Kawasaki disease; CI, confidence interval; Na+, sodium; LVEF, left ventricular ejection fraction; OR, odds ratio.

improved the AUC to 0.800. Model 3, which included Z-score, Na^+, LVEF, and myocardial T1 value, achieved a higher AUC of 0.851. Notably, Model 4, which also incorporated hepatic T1 value, demonstrated the highest AUC of 0.881. Significant improvements in AUC were observed for Model 3 and Model 4 compared to Model 1 (P=0.05 and P=0.01, respectively), with Model 4 also showing a significant enhancement over Model 2 (P=0.03). Although no statistical significance was observed between Models 1 and 2, Models 2 and 3, or Models 3 and 4, all models demonstrated increasing AUC values.

Intra- and inter-observer variability analysis

The intra- and inter-observer reliability of the measurement of the myocardial and hepatic T1 value showed good reproducibility, with the ICC ranging from 0.893 to 0.910 for myocardial T1 values and from 0.783 to 0.841 for hepatic T1 value in KD patients. Bland-Altman analysis revealed inter-observer agreement with mean bias of −1.79 ms (95% limits of agreement: −26.18 to 22.58 ms) for hepatic T1 mapping and −11.84 ms (95% limits of agreement: −72.17 to 48.49 ms) for cardiac T1 mapping (Figure S6).

Discussion

In KD patients, both cardiac and hepatic native T1 value were consistently elevated, suggesting a systemic response to inflammation. A positive correlation was observed between elevated hepatic and myocardial T1 value. CRP was an independent predictor of hepatic T1 value in the acute phase, whereas the disease phase and ALB correlated with hepatic T1 value across both phases. The LGE^+ subgroup

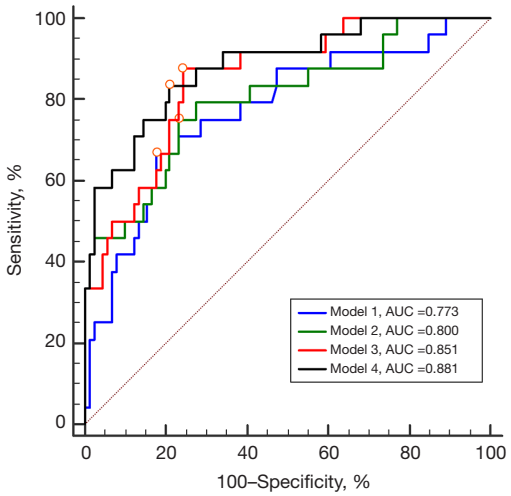

Figure 5 Comparison of ROC curves for different models. Model 1: Z-score + Na(+). Model 2: Z-score + Na(+) + LVEF. Model 3: Z-score + Na(+) + LVEF + myocardial T1. Model 4: Z-score + Na(+) + LVEF + myocardial T1 + hepatic T1. AUC, area under the curve; ROC, receiver operating characteristic; LVEF, left ventricular ejection fraction.

in each phase exhibited higher value compared to the LGE$^-$ subgroup. Logistic regression modeling indicated that a combined cardiac and hepatic T1 value could improve the diagnostic accuracy for myocardial LGE. These findings emphasize the intricate interplay between the systemic inflammatory response and myocardial and hepatic changes in KD, establishing a foundation for nuanced discussions on pathophysiology and potential therapeutic targets.

KD is recognized as a systemic disorder that primarily affects the cardiovascular system and mucocutaneous tissues; however, its hepatic implications are increasingly recognized (24). The elevated T1 value observed in both cardiac and hepatic issues during the acute phase of KD reflects the inflammatory milieu in our study, concurring with histopathological reports of cellular infiltration in these tissues (18,25). The distinct elevation of T1 value in acute KD (within 41 days) likely reflects an ongoing inflammatory response, corresponding to the histological evidence of inflammatory cell infiltration within myocardial tissues. At this early stage, these changes primarily represent active inflammation rather than established tissue remodeling—a phenomenon that subsides as the disease transitions to the chronic phase (26). Hepatic T1 alterations, particularly acute-phase elevations in our study, parallel autopsy findings where inflammation is histologically discerned in the portal tracts, bile ducts, and sinusoids, marked by lymphocytes and polymorphonuclear leukocytes as well as edematous changes. Although inflammation recedes in chronic KD, the persistence of elevated hepatic T1 value indicates a sustained, albeit attenuated, inflammatory process. This ongoing hepatic involvement, albeit milder, may have clinical implications and warrants further investigation into its pathophysiology and potential impact on KD management (3,4). It is important to note that at day 41, the elevated hepatic T1 values may still reflect ongoing inflammatory processes rather than established tissue changes. Longer-term follow-up studies would be needed to fully understand the evolution of these changes.

In recent years, the clinical application of native T1 value has become increasingly prevalent for liver assessment. Recent studies have demonstrated the potential utility of "native T1 value" as a diagnostic tool for liver fibrosis and as a predictor of clinical outcomes in patients with chronic liver diseases (27-29). For instance, de Lange *et al.* demonstrated that the assessment of native T1 value serves as a valuable tool for evaluating hepatic fibrosis and congestion in pediatric Fontan patients (16), whereas other research has confirmed its effectiveness in evaluating congestive hepatopathy in a broader patient population (30). Advances in CMR technology have facilitated the simultaneous quantification of myocardial and hepatic T1 value, enhancing the diagnosis of systemic diseases (31). Our results show that CRP, a marker synthesized by the liver with potential anti-inflammatory properties, serves as an independent predictor of hepatic T1 value during the acute phase (27). This suggests that elevated CRP levels, reflective of acute inflammation, may therefore impact upon hepatic T1 metrics, offering a non-invasive proxy for inflammatory status in KD (28,29). Our findings also demonstrated a consistent correlation between ALB level and hepatic T1 value across the disease continuum, affirming the protein's potential as a biomarker for hepatic integrity. Given the established relationship between serum ALB, IVIG resistance, and the development of CA lesions in KD (32,33), our analysis suggests ALB may serve as an indicator of systemic inflammation and hepatic histological alterations. Our findings advance the discourse on KD, postulating that the heightened inflammatory milieu in acute KD is palpable through elevated hepatic T1 value, with ALB levels serving as a concurrent gauge of this systemic response. As KD matures into its chronic phase, the decrement in inflammatory cell infiltration is mirrored by a reduction in T1 value, aligning with reported trends in hepatic function

markers.

LGE plays a significant role in the diagnosis and prognosis of nonischemic cardiomyopathy and myocarditis (34,35). In our study, we investigated the relationship between myocardial and hepatic T1 value and LGE in KD patients, adjusting for clinical features and laboratory markers. Our analysis revealed a significant and independent association between Z-score and Na^+ levels with myocardial LGE. The Z-score serves as an indicator of CA dilation, which, when prolonged, can result in impaired microcirculation, myocardial ischemia, and subsequent fibrosis (36,37). Previous studies have provided evidence supporting the relationship between sodium levels and vascular injury (38,39). Notably, hyponatremia, a common condition in KD patients, may promote endothelial damage and myocardial ischemia, potentially leading to LGE (40,41). Adding LVEF improved diagnostic accuracy, as it consistently correlates with LGE in myocarditis and dilated cardiomyopathy (42,43). Incorporating myocardial and hepatic T1 value further enhanced diagnostic performance, as elevated myocardial native T1 value are associated with myocardial LGE due to increased extracellular space (44-46). Given that KD primarily affects small- and medium-sized blood vessels throughout the body, individuals with more severe myocardial inflammation may also demonstrate liver inflammation or fibrosis. Histopathological analyses of endomyocardial biopsies and autopsies conducted on patients with chronic KD consistently demonstrate widespread fibrotic alterations and long-lasting myocardial inflammation (47,48). Although histopathological analyses have shown various myocardial changes in KD patients, it is important to note that in our cohort, the LGE findings at this early time point (41 days) likely represent active inflammation rather than established fibrosis. The correlation between T1 values and LGE is likely due to their shared underlying inflammatory mechanism rather than permanent tissue alterations. Combining MR histological information (myocardial and hepatic T1 value) significantly improved the diagnosis of myocardial LGE, offering a non-contrast method for assessing myocardial injury. Overall, the combination of myocardial and hepatic tissue analysis greatly enhances the accuracy of diagnosing myocardial LGE in KD.

Limitations

Several important limitations should be considered when interpreting our results. Firstly, this study employed a cross-sectional design to measure the T1 value in KD patients across both acute and chronic phases separately. However, due to the limited number of patients undergoing regular follow-up, it is crucial to investigate longitudinal changes in T1 value within the same patient from the acute phase to the chronic phase. Secondly, this research was conducted at a single center, using equipment from a single vendor and at a single magnetic field strength, which may limit the generalizability of the findings. The observed incidence of CA sequelae and resistance to IVIG was higher than the rates described in the AHA guideline, suggesting the need for multicenter studies to validate and strengthen our result. Thirdly, we performed imputation for the missing laboratory data, and although we employed imputation methods that maintained consistency before and after imputation, prospective and comprehensive data collection is necessary to provide a more comprehensive reflection of patients' laboratory profiles. The absence of cardiac enzyme data limits our ability to correlate T1 values with conventional biomarkers of myocardial injury. Additionally, a comprehensive multimodal assessment incorporating echocardiography and electrocardiography could provide more insights into the relationship between tissue characteristics and cardiac function. Future prospective studies should aim to integrate multiple diagnostic approaches, including cardiac biomarkers, various imaging modalities, and longitudinal follow-up, to better understand the complex pathophysiology of KD and its impact on multiple organ systems. Moreover, neither myocardial nor hepatic biopsy was performed to definitively confirm the presence of myocardial and hepatic injury in KD patients; further investigation is necessary to determine the clinical significance of elevated T1 value in KD patients. Future studies could benefit from integrating artificial intelligence technologies for automated image analysis to improve reproducibility and standardization, although our current methodology using experienced clinician interpretation and standardized protocols has demonstrated reliable results in evaluating cardiac and hepatic involvement in KD.

Conclusions

Our study demonstrates significant insights into the systemic manifestations of KD through comprehensive T1 mapping evaluation. The concurrent elevation of cardiac and hepatic T1 values, along with their positive correlation, provides strong evidence for multi-organ involvement in KD. The identification of CRP as an independent

predictor of hepatic T1 value in the acute phase, together with the associations between disease phase, ALB levels, and hepatic T1 value, enhances our understanding of disease progression. Most importantly, the integration of cardiac and hepatic T1 mapping offers several potential clinical applications: (I) improved diagnostic accuracy for myocardial involvement when combined with LGE assessment; (II) non-invasive evaluation of systemic inflammation; and (III) potential early recognition of organ involvement. These findings support the implementation of a comprehensive imaging approach in KD management, which may facilitate more accurate risk stratification and tailored therapeutic strategies.

Acknowledgments

None.

Footnote

Reporting Checklist: The authors have completed the STROBE reporting checklist. Available at https://qims.amegroups.com/article/view/10.21037/qims-24-791/rc

Funding: This work was supported by the National Natural Science Foundation of China (Nos. 82120108015, 82271981, 82471970, 82402250, 82402251, 82402249, 82304078, 82302168, and 824B2052), Sichuan Science and Technology Program (Nos. 23ZDYF2519, 2023NSFSC1715, 2024NSFSC0652, 2024YFFK0257, 2024YFFK0258, 2025ZNSFSC1772, and 2025ZNSFSC1767), Clinical Research Finding of Chinese Society of Cardiovascular Disease (CSC) of 2019 (No. HFCSC2019B01), Postdoctoral Fellowship Program of CPS Funder Grant (No. GZC20231830), Beijing Medical Award Foundation (No. 24H1187), and Sichuan University Interdisciplinary Innovation Fund, Chengdu Science and Technology program (No. 2024-YF05-02012-SN).

Conflicts of Interest: All authors have completed the ICMJE uniform disclosure form (available at https://qims.amegroups.com/article/view/10.21037/qims-24-791/coif). M.C. was an employee of Siemens Healthineers, Chengdu, China throughout his involvement in the study. The other authors have no conflicts of interest to declare.

Ethical Statement: The authors are accountable for all aspects of the work in ensuring that questions related to the accuracy or integrity of any part of the work are appropriately investigated and resolved. This study was conducted in accordance with the Declaration of Helsinki (as revised in 2013) and approved by the Ethics Committee of Sichuan University (No. K2019058). Written informed consent was provided by each patient's legal guardian before enrollment.

References

1. Burns JC. The etiologies of Kawasaki disease. J Clin Invest 2024;134:e176938.
2. Fukazawa R, Kobayashi J, Ayusawa M, et al. JCS/JSCS 2020 Guideline on Diagnosis and Management of Cardiovascular Sequelae in Kawasaki Disease. Circ J 2020;84:1348-407.
3. Ohshio G, Furukawa F, Fujiwara H, et al. Hepatomegaly and splenomegaly in Kawasaki disease. Pediatr Pathol 1985;4:257-64.
4. Amano S, Hazama F, Kubagawa H, et al. General pathology of Kawasaki disease. On the morphological alterations corresponding to the clinical manifestations. Acta Pathol Jpn 1980;30:681-94.
5. Dang Y, Hou Y. The prognostic value of late gadolinium enhancement in heart diseases: an umbrella review of meta-analyses of observational studies. Eur Radiol 2021;31:4528-37.
6. Dweck MR, Joshi S, Murigu T, et al. Midwall fibrosis is an independent predictor of mortality in patients with aortic stenosis. J Am Coll Cardiol 2011;58:1271-9.
7. Disertori M, Rigoni M, Pace N, Casolo G, Masè M, Gonzini L, Lucci D, Nollo G, Ravelli F. Myocardial Fibrosis Assessment by LGE Is a Powerful Predictor of Ventricular Tachyarrhythmias in Ischemic and Nonischemic LV Dysfunction: A Meta-Analysis. JACC Cardiovasc Imaging 2016;9:1046-55.
8. Dawson DK, Hawlisch K, Prescott G, et al. Prognostic

role of CMR in patients presenting with ventricular arrhythmias. JACC Cardiovasc Imaging 2013;6:335-44.
9. Grigoratos C, Di Bella G, Aquaro GD. Diagnostic and prognostic role of cardiac magnetic resonance in acute myocarditis. Heart Fail Rev 2019;24:81-90.
10. Muthusami P, Luining W, McCrindle B, et al. Myocardial Perfusion, Fibrosis, and Contractility in Children With Kawasaki Disease. JACC Cardiovasc Imaging 2018;11:1922-4.
11. Haaf P, Garg P, Messroghli DR, et al. Cardiac T1 Mapping and Extracellular Volume (ECV) in clinical practice: a comprehensive review. J Cardiovasc Magn Reson 2016;18:89.
12. Baskin KK, Bookout AL, Olson EN. The heart-liver metabolic axis: defective communication exacerbates disease. EMBO Mol Med 2014;6:436-8.
13. Hernandez-Anzaldo S, Berry E, Brglez V, Leung D, Yun TJ, Lee JS, Filep JG, Kassiri Z, Cheong C, Lambeau G, Lehner R, Fernandez-Patron C. Identification of a Novel Heart–Liver Axis: Matrix Metalloproteinase-2 Negatively Regulates Cardiac Secreted Phospholipase A2 to Modulate Lipid Metabolism and Inflammation in the Liver. J Am Heart Assoc 2015;4:e002553.
14. Correale M, Tarantino N, Petrucci R, et al. Liver disease and heart failure: Back and forth. Eur J Intern Med 2018;48:25-34.
15. Huber AT, Razakamanantsoa L, Lamy J, et al. Multiparametric Differentiation of Idiopathic Dilated Cardiomyopathy With and Without Congestive Heart Failure by Means of Cardiac and Hepatic T1-Weighted MRI Mapping. AJR Am J Roentgenol 2020;215:79-86.
16. de Lange C, Reichert MJE, Pagano JJ, et al. Increased extracellular volume in the liver of pediatric Fontan patients. J Cardiovasc Magn Reson 2019;21:39.
17. Wang J, Diao Y, Xu Y, et al. Liver T1 Mapping Derived From Cardiac Magnetic Resonance Imaging: A Potential Prognostic Marker in Idiopathic Dilated Cardiomyopathy. J Magn Reson Imaging 2024;60:675-85.
18. Harada M, Yokouchi Y, Oharaseki T, et al. Histopathological characteristics of myocarditis in acute-phase Kawasaki disease. Histopathology 2012;61:1156-67.
19. Hu L, A-Zhe SG, Zhou ZQ, et al. Quantitative Assessment of Myocardial Edema by MR T2 Mapping in Children With Kawasaki Disease. J Magn Reson Imaging 2024;59:825-34.
20. Cornicelli MD, Rigsby CK, Rychlik K, et al. Diagnostic performance of cardiovascular magnetic resonance native T1 and T2 mapping in pediatric patients with acute myocarditis. J Cardiovasc Magn Reson 2019;21:40.
21. Zhou Z, Wei D, Azhe S, et al. Self-navigated coronary MR angiography for coronary aneurysm detection in Kawasaki disease at 3T: comparison with conventional diaphragm-navigated coronary MR angiography. Eur Radiol 2024;34:3400-10.
22. Le MTP, Zarinabad N, D'Angelo T, et al. Sub-segmental quantification of single (stress)-pass perfusion CMR improves the diagnostic accuracy for detection of obstructive coronary artery disease. J Cardiovasc Magn Reson 2020;22:14.
23. Kobayashi T, Fuse S, Sakamoto N, et al. A New Z Score Curve of the Coronary Arterial Internal Diameter Using the Lambda-Mu-Sigma Method in a Pediatric Population. J Am Soc Echocardiogr 2016;29:794-801.e29.
24. Zhou Z, Zhang N, Azhe S, et al. Myocardial perfusion impairment in children with Kawasaki disease: assessment with cardiac magnetic resonance first-pass perfusion. Quant Imaging Med Surg 2024;14:4923-35.
25. Eladawy M, Dominguez SR, Anderson MS, et al. Abnormal liver panel in acute kawasaki disease. Pediatr Infect Dis J 2011;30:141-4.
26. Liu AM, Ghazizadeh M, Onouchi Z, et al. Ultrastructural characteristics of myocardial and coronary microvascular lesions in Kawasaki disease. Microvasc Res 1999;58:10-27.
27. Ramachandran P, Serai SD, Veldtman GR, et al. Assessment of liver T1 mapping in fontan patients and its correlation with magnetic resonance elastography-derived liver stiffness. Abdom Radiol (NY) 2019;44:2403-8.
28. Banerjee R, Pavlides M, Tunnicliffe EM, et al. Multiparametric magnetic resonance for the non-invasive diagnosis of liver disease. J Hepatol 2014;60:69-77.
29. Pavlides M, Banerjee R, Sellwood J, et al. Multiparametric magnetic resonance imaging predicts clinical outcomes in patients with chronic liver disease. J Hepatol 2016;64:308-15.
30. Kazour I, Serai SD, Xanthakos SA, et al. Using T1 mapping in cardiovascular magnetic resonance to assess congestive hepatopathy. Abdom Radiol (NY) 2018;43:2679-85.
31. Meloni A, Carnevale A, Gaio P, et al. Liver T1 and T2 mapping in a large cohort of healthy subjects: normal ranges and correlation with age and sex. MAGMA 2024;37:93-100.
32. Yan Y, Qiao L, Hua Y, et al. Predictive value of Albumin-Bilirubin grade for intravenous immunoglobulin resistance in a large cohort of patients with Kawasaki disease: a prospective study. Pediatr Rheumatol Online J

2021;19:147.
33. Xia Y, Qiu H, Wen Z, et al. Albumin level and progression of coronary artery lesions in Kawasaki disease: A retrospective cohort study. Front Pediatr 2022;10:947059.
34. Di Marco A, Anguera I, Schmitt M, Klem I, Neilan TG, White JA, Sramko M, Masci PG, Barison A, Mckenna P, Mordi I, Haugaa KH, Leyva F, Rodriguez Capitán J, Satoh H, Nabeta T, Dallaglio PD, Campbell NG, Sabaté X, Cequier Á. Late Gadolinium Enhancement and the Risk for Ventricular Arrhythmias or Sudden Death in Dilated Cardiomyopathy: Systematic Review and Meta-Analysis. JACC Heart Fail 2017;5:28-38. Erratum in: JACC Heart Fail 2017;5:316.
35. Gräni C, Eichhorn C, Bière L, et al. Prognostic Value of Cardiac Magnetic Resonance Tissue Characterization in Risk Stratifying Patients With Suspected Myocarditis. J Am Coll Cardiol 2017;70:1964-76.
36. Friesen RM, Schäfer M, Jone PN, et al. Myocardial Perfusion Reserve Index in Children With Kawasaki Disease. J Magn Reson Imaging 2018;48:132-9.
37. Bratis K, Chiribiri A, Hussain T, et al. Abnormal myocardial perfusion in Kawasaki disease convalescence. JACC Cardiovasc Imaging 2015;8:106-8.
38. Lima CT, Silva JC, Viegas KA, et al. Increase in Vascular Injury of Sodium Overloaded Mice May be Related to Vascular Angiotensin Modulation. PLoS One 2015;10:e0128141.
39. Pacurari M, Kafoury R, Tchounwou PB, et al. The Renin-Angiotensin-aldosterone system in vascular inflammation and remodeling. Int J Inflam 2014;2014:689360.
40. Park S, Eun LY, Kim JH. Relationship between serum sodium level and coronary artery abnormality in Kawasaki disease. Korean J Pediatr 2017;60:38-44.
41. Miura K, Harita Y, Takahashi N, et al. Nonosmotic secretion of arginine vasopressin and salt loss in hyponatremia in Kawasaki disease. Pediatr Int 2020;62:363-70.
42. Bohbot Y, Garot J, Hovasse T, et al. Clinical and Cardiovascular Magnetic Resonance Predictors of Early and Long-Term Clinical Outcome in Acute Myocarditis. Front Cardiovasc Med 2022;9:886607.
43. Habib M, Adler A, Fardfini K, Hoss S, Hanneman K, Rowin EJ, Maron MS, Maron BJ, Rakowski H, Chan RH. Progression of Myocardial Fibrosis in Hypertrophic Cardiomyopathy: A Cardiac Magnetic Resonance Study. JACC Cardiovasc Imaging 2021;14:947-58.
44. Li Y, Xu Y, Li W, et al. Cardiac MRI to Predict Sudden Cardiac Death Risk in Dilated Cardiomyopathy. Radiology 2023;307:e222552.
45. Eichhorn C, Greulich S, Bucciarelli-Ducci C, et al. Multiparametric Cardiovascular Magnetic Resonance Approach in Diagnosing, Monitoring, and Prognostication of Myocarditis. JACC Cardiovasc Imaging 2022;15:1325-38.
46. Li S, Zhou D, Sirajuddin A, He J, Xu J, Zhuang B, Huang J, Yin G, Fan X, Wu W, Sun X, Zhao S, Arai AE, Lu M. T1 Mapping and Extracellular Volume Fraction in Dilated Cardiomyopathy: A Prognosis Study. JACC Cardiovasc Imaging 2022;15:578-90.
47. Pilania RK, Jindal AK, Bhattarai D, et al. Cardiovascular Involvement in Kawasaki Disease Is Much More Than Mere Coronary Arteritis. Front Pediatr 2020;8:526969.
48. Yutani C, Go S, Kamiya T, et al. Cardiac biopsy of Kawasaki disease. Arch Pathol Lab Med 1981;105:470-3.

Cite this article as: Peng S, Wen L, Zhou Z, Huang S, Hu L, Azhe S, Wang C, Zhang N, Chen M, Zhou K, Guo Y. Correlation between cardiac and hepatic native T1 value and myocardial late gadolinium enhancement in children with Kawasaki disease. Quant Imaging Med Surg 2025;15(3):1990-2002. doi: 10.21037/qims-24-791